ZAMM · Z. Angew. Math. Mech. **95**, No. 8, 822 – 830 (2015) / **DOI** 10.1002/zamm.201300300

Friction between a rigid body and a model elastomer having a linear viscous rheology

Silvio Kürschner*

Berlin University of Technology, 10623 Berlin, Germany

Received 20 December 2013, revised 3 March 2014, accepted 24 April 2014
Published online 19 May 2014

Key words Viscoelasticity, rheological modeling, coefficient of friction.

The present paper contributes to the modeling of contacts with viscoelastic materials. An indenter is pressed into an elastomer and slides on its surface with a constant velocity. Contact regions typically experience periodical loading due to surface roughness with characteristic length scales. Loading within a medium frequency range is studied, in which the viscous properties of the elastomer dominate. After passing a transition zone a stationary state is reached. An one-dimensional model is used to determine estimations for the indentation depth and the coefficient of friction. Results for two simply shaped indenters are presented and compared to boundary element simulations.

1 Introduction

Elastomers are widely used in tribological applications. They provide high frictional forces and sustain large deformations. These properties are utilized in different domains of technology. In comparison to linear elastic materials their behavior is hard to describe. This is based on the existence of viscous and elastic properties side by side. Therefore this class of material behavior is called viscoelasticity. Since the modeling of these materials is researched for more than half a century [9], it is still a work in progress as current studies [2, 22] demonstrate.

The main difference between purely elastic and viscoelastic characteristics can easily be demonstrated in terms of the stress-strain-relations [11]. Linear elastic materials are characterized by Hooke's law. For the sake of clarity, we survey Hooke's law in shear: $\sigma = 2G\varepsilon$. The stress σ is proportional to the strain ε, with G being the shear modulus. For a viscoelastic material the same relation reads:

$$\sigma(t) = 2\int_{\tau=-\infty}^{t} G(t-\tau)\frac{\partial}{\partial\tau}\varepsilon(\tau)\mathrm{d}\tau, \tag{1}$$

where $G(t)$ is the relaxation function in shear [3].

If an elastomer is loaded periodically with a characteristic frequency, one can often estimate its behavior. Such characteristic frequencies appear regularly in contact problems. Let us assume two bodies are brought in contact and slide against each other with the velocity v. If one body has a rough surface with a characteristic wavelength λ, the deformation of the surface features occurs with a frequency $\omega \approx \frac{v}{\lambda}$.

In this case, the relaxation function (1) is a complex function in the frequency domain: the complex shear modulus. Its real part describes the stored elastic energy and is therefore called the storage modulus $G'(\omega)$. The imaginary part is related to the dissipative processes and is termed the loss modulus $G''(\omega)$. The quotient of loss and storage modulus is sometimes called loss tangent $\tan\delta(\omega) = G''(\omega)/G'(\omega)$. It describes the ratio of dissipative and elastic effects.

The frequency dependent behavior of many typical elastomers can be qualitatively depicted as follows: In the case of very low frequencies $\omega \to 0$, most elastomers behave like an elastic material with a small modulus of elasticity. The same holds for loading with very high frequencies $\omega \to \infty$, but the elastic modulus is much higher than the first one, typically three or four orders of magnitude. In both cases almost no dissipation appears and the loss tangent is close to zero. In contrast, in a medium frequency range, the loss tangent can be close to unity or even larger. In this case elastomers typically behave like a viscous fluid [3, 19].

The simplest model which covers this characteristic is a generalized Maxwell model involving a spring (stiffness G_1) in parallel to another spring (stiffness G_2) and a dashpot (viscosity η) in series as shown in the lower right corner of Fig. 1.

* E-mail: si.kuerschner@gmail.com, Phone: +49 30 314 23454, Fax: +49 30 314 72575

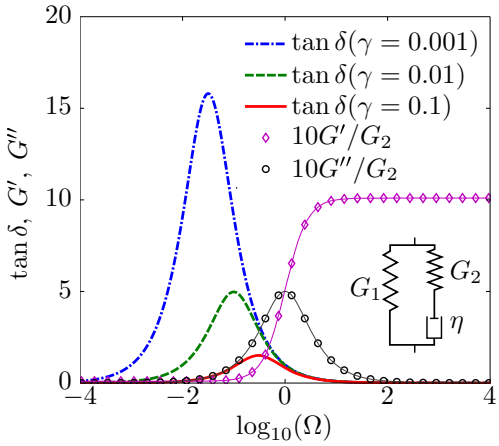

Fig. 1 The loss tangent $\tan\delta$ as a function of the dimensionless frequency $\Omega = \omega G_2/\eta$ for three different ratios $\gamma := G_1/G_2 = 1/1000$ (blue dash-dot line), $1/100$ (green broken line), $1/10$ (red solid line). The thin magenta line marked by diamonds shows the storage modulus and the thin black line marked by circles the loss modulus. Both are based on $\gamma = 1/100$ and are scaled by a factor of $10/G_2$ for better perceptibility. The model is shown in the lower right corner.

One can easily calculate storage modulus, loss modulus, and loss tangent of this model:

$$G'(\Omega) = G_2\left(\gamma + \frac{\Omega^2}{1+\Omega^2}\right), \quad G''(\Omega) = G_2\frac{\Omega}{1+\Omega^2}, \quad \tan\delta(\Omega) = \frac{\Omega}{\Omega^2 + \gamma(1+\Omega^2)}, \tag{2}$$

with $\Omega := \omega G_2/\eta$ and $\gamma := G_1/G_2$ being the dimensionless frequency and the ratio of stiffness parameters, respectively [19]. Remarkably, the three functions do not depend on the viscosity directly but on the ratio Ω only. Thus, a change of viscosity causes a shifting along the Ω-axis. The loss tangent depends on the dimensionless parameters Ω and γ only.

In Fig. 1 the loss tangent of this model is shown for three different stiffness ratios $\gamma = 1/1000,\ 1/100,\ 1/10$. Additionally, storage and loss moduli are shown for $\gamma = 1/100$. They are scaled by a factor $10/G_2$ for better perceptibility. While these are the results of a simple model, they qualitatively agree with general considerations (cf. [3], Fig. 1.7) and experimental studies (cf. [17], Fig. 19)[1].

The behavior within the elastic limits, $\Omega \to 0$ and $\Omega \to \infty$, is widely studied (e.g. [7]) due to practical applications. This is not the case for the domain between these limits, in which the viscous properties significantly influence or even dominate the properties.

The present paper contributes to elastomer-contacts within this viscosity dominated domain. The elastic-like part and the crossover between elastic and viscous behavior are not in the scope of this study. Thus, the results are valid in a medium frequency range only. They do not hold for very low and very high (dimensionless) frequencies.

This paper has two major aims. An analytic estimation of the behavior within the domain of high dissipation is provided and supported by the boundary element method. But the approach itself is widely independent of the rheological model and can be applied to even more realistic ones. Thus, the second aim is to create a basis for further works for a better understanding and estimation of friction of elastomers.

To do so, the tribological setup is described in more detail in Sect. 2. Two approaches are used to study the current problem: the method of dimensionality reduction and the boundary element method. Both are briefly described in Sect. 3. The stationary indentation depth and the stationary coefficient of friction are deduced analytically based on the method of dimensionality reduction in Sect. 4. Finally, the results are compared to boundary elements simulations in Sect. 5.

2 Contact with a viscous half space

We consider a contact problem between an indenter and an elastomer. The first is considered to be rigid and much smaller than the latter. Therefore, the whole surface topography is ascribed to the indenter. The elastomer is treated as a half space with an originally flat surface. The half space assumption implies small deformations and small surface gradients at least in the contact area. Additionally it ensures that the elastomer can be pressed downwards (to infinity).[2]

We study the medium frequency range mentioned in Sect. 1. Therefore, the elastomer is modeled as a linearly viscous isotropic and homogeneous material. For simplicity, incompressibility is assumed and inertia effects are neglected. Adhesion is not in the scope of this study. The shear stresses σ are related to the deformation rates $\dot{\varepsilon}$ via

$$\sigma = 2\eta\dot{\varepsilon}, \tag{3}$$

[1] In experimental studies as the cited one the viscoelastic properties are often related to temperature variations instead of frequencies due to the experimental setup. But both approaches are closely connected via the master curve procedure [8].

[2] Therefore, the half space assumption is crucial. In particular, the model is not suitable for thin layers of elastomers, which have to dealt with in a different way, cf. [1].

where η is the viscosity and the dot marks differentiation with respect to time, $\dot{\varepsilon} = \frac{\partial}{\partial t}\varepsilon$.

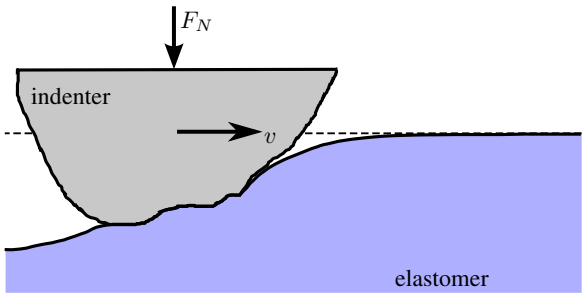

Fig. 2 The problem under study: An indenter is pressed into the elastomer and driven tangentially with a constant velocity v.

The indenter is loaded by a constant normal force F_N and moves horizontally with a constant velocity v. Firstly, it sinks into the elastomer. At a certain indentation depth, the vertical component of the interaction force between indenter and elastomer compensates the external force. The process becomes stationary and a final coefficient of friction μ can be defined as the ratio of the horizontal component F_h of the interaction force and the external force F_N,

$$\mu := \frac{F_h}{F_N}. \tag{4}$$

We consider the following boundary conditions on the surface of the half space: Within the contact area, the gap between indenter and elastomer vanishes, while elsewhere on the surface the normal stress is equal to zero. The whole surface is free of shear stresses. The last condition in connection with the half space assumption leads to an important conclusion: the horizontal component of the interaction force is much smaller than its vertical component at any given point on the contact area (Fig. 6). This can easily be shown by geometrical considerations. Therefore, we will neglect it and treat the problem as a normal contact at first. The horizontal force is calculated subsequently in accordance with the local surface gradients.

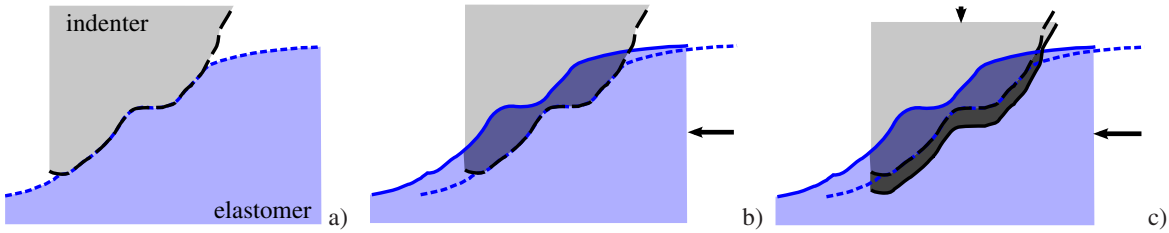

Fig. 3 **a)** Indenter and elastomer are brought into contact. Their surfaces are drawn with broken lines, which can be seen in the following figures as references. **b)** The elastomer is moved to the left. The darker volume of elastomer has to be squeezed downwards by the indenter. **c)** The indenter is shifted vertically to balance the external force by the vertical component of the interaction force. The grey colored volume of elastomer is additionally squeezed out.

The model works in the following way: Indenter and elastomer are brought into contact, Fig. 3a). The indenter is moved horizontally with the velocity v. Equivalently, the elastomer can be moved in the opposite direction. This was done due to implementation matters. Within regions where indenter and half space would overlap each other, the elastomer is squeezed downwards by surface stresses, Fig. 3b). In addition, the indenter is shifted vertically to meet the balance of forces, Fig. 3c).

As mentioned earlier, the frictional force is calculated subsequently by integrating the product of normal stress and surface gradient over the contact area. The coefficient of friction is evaluated as the ratio of frictional force and external force after reaching the stationary state.

3 Mathematical approaches

Two different mathematical approaches are used to study the current problem. Analytical and numerical consideration are performed on an one-dimensional model in accordance with the method of dimensionality reduction. The results are compared to boundary element simulations. While the assumptions of the tribological setup are considered within both approaches, the further assumption of the method of dimensionality reduction are not related to the boundary element method. In fact, both approaches are independent of each other.

By use of the boundary element method the further considerations are restricted to the surface of the elastomer. The number of spatial dimensions is decreased from three to two and the numerical complexity is strongly reduced. The surfaces

of elastomer and indenter are discretized into quadratic-shaped elements. Stress, deformation, and deformation velocity are constant within each element. The elements meet one of two possible boundary conditions. Within the contact area the gap between indenter and elastomer vanishes and a positive normal stress is applied. Outside of the contact area, the gap is positive but the normal stress vanishes.

Each element in contact induces a deformation velocity on all elements of the elastomer's surface which is determined by a discretized formulation of the Green's function [4]:

$$\dot{u}(r) = \frac{f}{4\pi\eta r}, \tag{5}$$

where r is the distance between the elements and f is the normal force on the element in contact. This formula can be obtained from the Green's function of the elastic contact [14],

$$u(r) = \frac{f}{4\pi G r}, \tag{6}$$

by Radok's principle of functional equations [15, 21] as shown in [12].

In every time-step, contact area, normal stress distribution, and deformation velocities are calculated iteratively. After that the indenter is moved as described in Sect. 2. Additionally, the surface deformations are updated by integrating the deformation velocities with respect to time.

The method of dimensionality reduction maps the three-dimensional system onto a one-dimensional one. The method was proposed by Popov and Psakhie [18] and applied to elastic contact problems at first [5, 6]. Recently, applications to viscous [12, 13] and Kelvin-type viscoelastic [16] contact problems have been published, too. The approach is described in more detail in a recent monograph [20].

Within the method of dimensionality reduction, the indenter is mapped onto a rigid line by a specific transformation rule. At present this rule is known for two types of indenters. On the one hand, indenters with self-affine, randomly rough surfaces can be transformed into statistically equivalent lines. The present study does not deal with this class of indenters. On the other hand, bodies of revolution with the shape of a power function,

$$h_p(r) = c_p r^p, \tag{7}$$

with p being a positive real number and c_p being a coefficient, can be mapped onto one dimensional lines[3] exactly. This still holds, under certain assumptions, for superpositions of different power functions. Based on Segedin [23] and Sneddon [24], Heß proved in his dissertation [10] that the equivalent line $\tilde{h}(x)$ can be constructed by

$$\tilde{h}_p(x) = \kappa_p c_p |x|^p. \tag{8}$$

The transformation parameter

$$\kappa_p \equiv \kappa(p) := \frac{\sqrt{\pi}}{2} \frac{p\Gamma\left(\frac{p}{2}\right)}{\Gamma\left(\frac{p+1}{2}\right)}, \tag{9}$$

stretches the surface to exactly meet the force-indentation-relation of normal contact, as proved in [10]. Γ denotes the Gammafunction, $\Gamma(x) = \int_0^\infty t^{x-1}\mathrm{e}^{-t}\mathrm{d}t$.

We will later consider two particular indenters. The first is a cone constructed by a linear function, $h_1(r) = c_1 r$ and the second is a paraboloid of revolution generated by $h_2(r) = c_2 r^2$. The transformation parameters are $\kappa_1 = \frac{\pi}{2}$ and $\kappa_2 = 2$, respectively.

The viscous half space is mapped onto a chain of independent dashpots, each connecting local force f and deformation velocity $\dot{u}$ by

$$f = 4\eta\Delta x\dot{u}, \tag{10}$$

where Δx is the spacing between two elements. In Fig. 4 the contact between a rigid paraboloid of revolution and a viscous half-space and the one-dimensional model are shown as an example.

The boundary element model and the one according to the method of dimensionality reduction were previously used to study normal contacts -without tangential movement- with axially symmetric [12] and with self-affine, randomly rough indenters [13].

While axis-symmetric indenters are in the focus of this section, the method of dimensionality reduction is not restricted to this kind of indenters or to axis-symmetric problems. This class of indenters is chosen because an exact transformation rule is known and unnecessary difficulties are avoided in the next section. However, this approach can be further generalized.

[3] The surface h of the original indenter is described by cylindrical coordinates $\{r, \varphi, z\}$. The surface $\tilde{h}$ of the one-dimensional model is termed line and described by Cartesian coordinates $\{x, z\}$.

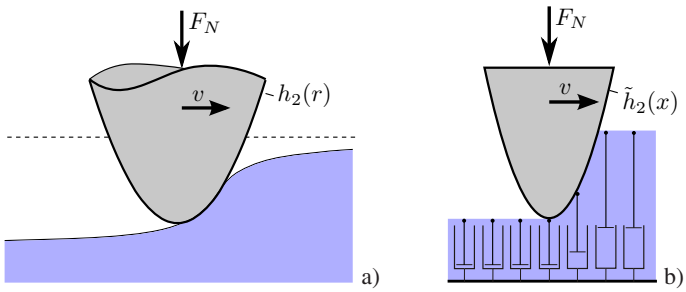

Fig. 4 **a)** The three-dimensional problem of a paraboloid of revolution which is pressed into a viscous half space and moved tangentially. **b)** The one-dimensional model according to the method of dimensionality reduction.

4 Analytical estimation of the coefficient of friction

In this section an analytical estimation of the coefficient of friction is deduced within the framework of the method of dimensionality reduction. Thus, the following considerations exactly hold for the artificial one-dimensional model.

We consider a rigid line which is pressed into a chain of independent dashpots, each having a characteristic as described in Eq. (10), due to a constant normal force F_N. Additionally, the line is moved horizontally by a constant velocity v.

Preliminarily we introduce the terms leading edge and contact line and prove a theorem, which delivers the stationary indentation depth. The latter one is meant to be the final indentation depth, at which the external force is exactly balanced by the vertical component of the interaction force between indenter and half space.

Definition 1 (leading edge)**.** Let X be a closed interval of the set of real numbers $\mathbb{R}$ and $\tilde{h} : X \mapsto \mathbb{R}$ a non-constant, continuous function. The leading edge A of $\tilde{h}$ is the subset $A := \{x \in X | \tilde{h}(x) < \tilde{h}(\xi), \forall \xi > x\} \subset X$.

Definition 2 (contact line)**.** With the assumptions and notions of definition 1 and a given number $d \leq \max_{x\in A} h(x)$, the contact line of $\tilde{h}$ (with respect to d) is the subset $A_d := \{x \in A | h(x) \leq d\} \subset A$. If $A_d \neq \emptyset$, it consists of intervals, $A_d = \bigcup_{i=1}^{n} A_i, n \in \mathbb{N}$, with $A_1 = [\alpha_1, \beta_1]$ and, if $n > 1$, $A_i = [\alpha_i, \beta_i[, 1 < i \leq n$. If f is a continuous function on A_d, we define:

$$\int_{A_d} f(x)\mathrm{d}x := \sum_{i=1}^{n} \int_{\alpha_i}^{\beta_i} f(x)\mathrm{d}x. \tag{11}$$

Theorem 3 (stationary indentation depth)**.** *Suppose $X \subset \mathbb{R}$ is a closed set and $\tilde{h} : X \mapsto \mathbb{R}, x \mapsto \tilde{h}(x)$ is a non-constant, continuous function describing a rigid line. The line is pressed into a chain of independent dashpots (the elastomer) with the characteristic described in Eq.* (10) *by a constant normal force F_N and is moved into positive direction of x with a constant velocity $v > 0$. The stationary indentation depth d, if it exists, is determined by*

$$d = \frac{F_N}{4\eta v}. \tag{12}$$

Proof. We suppose the final stationary state exists and the system has reached it. According to the model description in Sect. 2, each dashpot is in one of two states. Either it is free of force or a compressing stress acts on it. Under no circumstances do tensile stresses occur. This means a dashpot can only be compressed but never be extended. Therefore, if the system is in the stationary state and a force acts on a dashpot at a position $x \in X$, then it is a compressing stress and $x \in A$ holds with A being the leading edge of $\tilde{h}$. Contrariwise, if a position $x \in X$ is not in A, then no force acts on this position.

Since $\tilde{h}$ is continuous on A and on behalf of definition 1, the restriction $\tilde{h}_A := \tilde{h}|_A : A \mapsto \mathbb{R}$ is continuous and monotonically increasing on A. It is sufficient to study the restricted line $\tilde{h}_A$, Fig. 5.

On behalf of the construction of the function, $\tilde{h}_A$ has a global minimum, say h_0. Let $d > 0$ be the indentation depth, meaning that a point $x_d \in A$ with $\tilde{h}_A(x_d) = h_0 + d$ exists and a point $x \in A$ of the rigid line carries an interaction force if and only if $x \leq x_d$ holds. Thus, the contact line is $A_d = \{x \in A | x \leq x_d\}$.

Suppose the rigid line is shifted into positive direction (of x) by a distance l. This spans a period of time of $t = l/v$. The volume of elastomer enclosed between the curves $\tilde{h}(x)$, $\tilde{h}(x + l)$ and the parallels to the x-axis going through h_0 and $h_0 + d$ respectively is of the size $Q = ld$. This volume has to be squeezed out with a rate of $\dot{Q} = ld/t$. The specific squeeze out rate based on the dashpot width reads

$$\dot{q} = \frac{vd}{\Delta x}. \tag{13}$$

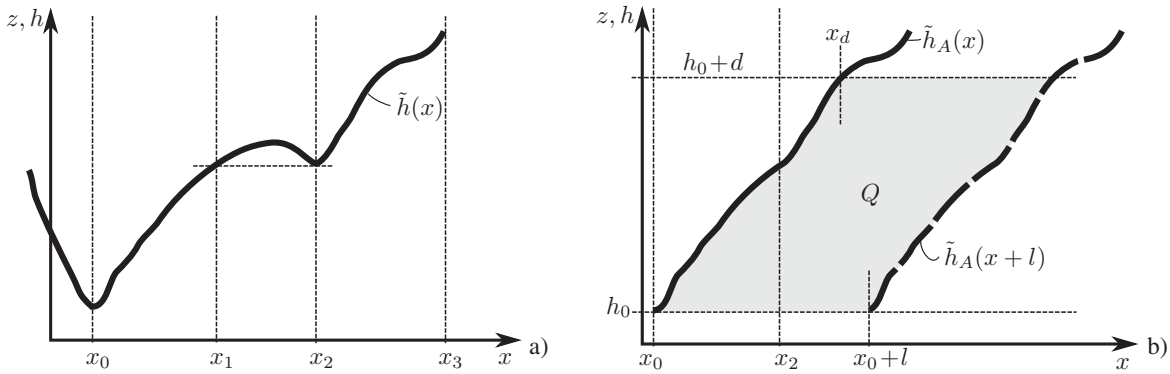

Fig. 5 **a)** The leading edge A of $\tilde{h}(x)$ is the subset $A := [x_0, x_1[\cup [x_2, x_3]$ of $\mathbb{R}$. The interval $[x_1, x_2[$ is not included in the leading edge. **b)** The indentation depth is d and the contact line is the subset $A_d = [x_0, x_1[\cup [x_2, x_d]$ of A. The volume Q of elastomer to be squeezed out is bounded by the restricted function $\tilde{h}_A(x)$, its shifted copy $\tilde{h}_A(x+l)$ and the horizontal lines $z = h_0$ and $z = h_0 + d$.

This quantity accords with the deformation rate, if the whole volume Q would be squeezed out over the width of one dashpot. Equation (10) delivers the required force F to produce this squeeze out rate:

$$F = 4\eta d v. \tag{14}$$

We remark that the dashpots are independent of each other and their characteristic (10) is linear. Therefore, the result (14) is valid for the case that the elastomer is distributed over several dashpots, too. Since the system is in a stationary state, the interaction force F is equal to the external force F_N. Thus, Eq. (14) gives the stationary indentation depth as stated above. □

Remark 4. We supposed that a final stationary state exists. If it does not exist it is because a point x_d with the property $\tilde{h}_A(x_d) = h_0 + d$ does not exists on the leading edge A. One can mention two possible reasons for this. Firstly, the indenter's height is too small (smaller than d) to reach the stationary state. In this case, a final stationary state really does not exist, based on the chosen parameters. Secondly, the indenter is high enough, but the leading edge is not. This is related to the mathematical formulation only and can not happen with real indenters.

Remark 5. We unnecessarily assumed the system to be in a stationary state. The same considerations can be done without that assumption. They deliver the instantaneous indentation velocity

$$v_z = \frac{F_N}{4\eta a} - \frac{v d}{a}, \tag{15}$$

with d being the present indentation depth, $a = n_c \Delta x$ the projected contact length and n_c is the number of dashpots in contact. Since we will not use this result and the proof is more cumbersome than the one above, it is not provided here.

We can now state the main result of this section.

Theorem 6 (stationary coefficient of friction)**.** *With the assumptions of Theorem* 3 *and* $\tilde{h}$ *being continuously differentiable, the coefficient of friction* μ *in the final stationary state, if it exists, is determined by*

$$\mu = \frac{4\eta v}{F_N} \int_{A_d} (\tilde{h}'(x))^2 \mathrm{d}x. \tag{16}$$

P r o o f. In reference to Fig. 6, we consider an arbitrary point $x_0 \in A_d$ of the contact line with the property $\tilde{h}(x_0) = h_0$. We suppose the indenter is shifted into positive direction (of x) by a small distance $\xi > 0$ with $[x_0, x_0 + \xi[\subset A_d$ and $\tilde{h}(x_0 + \xi) = h_0 + \zeta$. During this time span, $\Delta t = \xi / v$, the elastomer at the position x_0 has to be squeezed out by an amount of ζ into negative direction of z. The squeeze out rate is $\dot{z}(x_0) = -\frac{\zeta}{\xi} v$. Since ξ is small, $\lim_{\xi \to 0} \frac{\zeta}{\xi} = \tilde{h}'(x_0)$ holds and therefore we can write

$$\dot{z} = -\tilde{h}'(x_0) v. \tag{17}$$

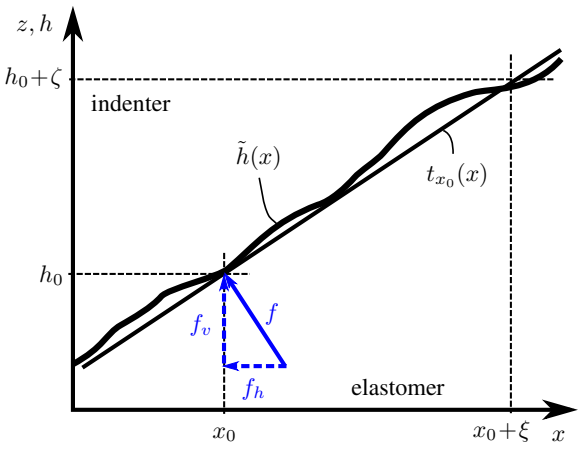

Fig. 6 The local frictional force: The rigid line $\tilde{h}$ is moved by a small distance ξ in positive x-direction. During this time the elastomer has to be squeezed out over the height ζ. For this the force f_v is needed. The interaction force f itself is perpendicular to the tangent t_{x_0} on $\tilde{h}$ in x_0 as described in Sect. 2. Thus, the gradient $\tilde{h}'(x_0)$ determines the ratio f_h/f_v.

To induce this squeeze out rate, the local force f_v on the elastomer's surface has to be

$$f_v(x_0) = 4\eta v \tilde{h}'(x_0)\xi, \tag{18}$$

in accordance with Eq. (10). The vertical component of the local force acting on the rigid line at x_0 has the same value but points in the opposite direction.

As mentioned in Sect. 2 the treatment as a pure normal contact is dropped now. According to the premise of zero shear stresses, the interaction force $f(x_0)$ is perpendicular to the tangent $t_{x_0}(x) := h_0 + h'(x_0)(x - x_0)$ on $\tilde{h}$ in x_0. Thus, we obtain the local frictional force $f_h(x_0) = f_v(x_0)h'(x_0)$ and from Eq. (18):

$$f_h(x_0) = 4\eta v(\tilde{h}'(x_0))^2\xi. \tag{19}$$

The continuum limit delivers the differential frictional force:

$$\mathrm{d}F_h(x) = \lim_{\xi \to \mathrm{d}x} f_h(x) = 4\eta v(\tilde{h}'(x))^2 \mathrm{d}x. \tag{20}$$

We obtain the stationary coefficient of friction via integration of all differential frictional forces and dividing the result by the external force. According to Theorem 3, the indentation depth is d and the interaction force is distributed over the contact line A_d. Thus, we finally obtain the coefficient of friction as stated above. □

5 Results

In Sect. 4 was shown that the results of Theorem 6 hold exactly regarding the one-dimensional model. Furthermore, they deliver proper estimations in reference to the original three-dimensional system. Proper refers to a reasonable dimensional analysis and it differs by a constant factor of the order of unity only. These considerations, of course, are based on the premise that the construction rule for the one-dimensional model is known. As mentioned earlier, we do not claim to know a proper construction for every imaginable indenter.

In this section we compare the analytical results with such obtained numerically by the boundary element method. Additionally, we provide results from a numerical simulation with the method of dimensionality reduction. While both methods meet the assumptions as described in Sect. 2, they differ in relation to other properties.

Two specific types of axially symmetric indenters are studied, a cone and a paraboloid of revolution. The first one is constructed by rotating the positive part of a straight line $h_1(r) = c_1 r$ around the origin $r = 0$. As described in Sect. 3 the equivalent one-dimensional indenter is represented by the function $\tilde{h}_1(x) = \frac{\pi}{2} c_1 |x|$.[4] We suppose a given set of parameters: External force F_N, horizontal velocity v, viscosity η, and gradient c_1. The stationary indentation depth d, the contact line A_d, and the coefficient of friction μ read:

[4] Since $\tilde{h}_1$ is not continuously differentiable in $x = 0$, we restrict $\tilde{h}_1$ and it's derivative $\tilde{h}_1'$ to the set $x \geq 0$ (read: the leading edge) and continuously extend $\tilde{h}_1'$ by explicitly defining $\tilde{h}_1'(0) := \frac{\pi}{2} c_1$.

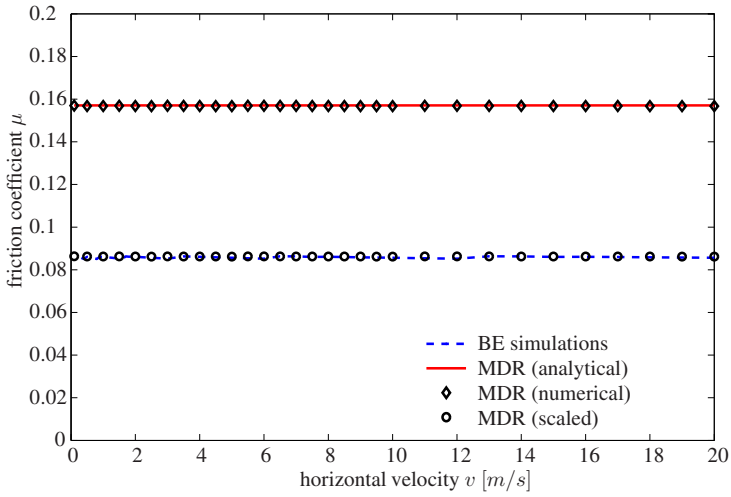

Fig. 7 Comparison of the results obtained by the method of dimensionality reduction (MDR) and by boundary element (BE) simulations. The diagram shows the coefficient of friction as a function of horizontal velocity in the case of a cone-shaped indenter. The results differ by a constant factor only. Thus, the one-dimensional results, scaled by a constant factor of $s_1 \approx 0.55$, nearly coincide with the BE-simulations.

$$d = \frac{F_N}{4\eta v}, \quad A_d = \left[0, \frac{F_N}{2\pi c_1 \eta v}\right], \quad \mu = \frac{\pi}{2} c_1, \tag{21}$$

according to Eq. (12), the indenter's geometry, and Eq. (16), respectively.

This provides a basic result: the coefficient of friction depends on the gradient c_1 only. This is supported by numerical simulations with the same model. In Fig. 7 the results are plotted as functions of velocity for a given value $c_1 = 0.1$. As one can see, they are constant lines with small perturbations due to discretization errors. The results by the method of dimensionality reduction differ from the boundary element simulations by a constant factor of $s_1 \approx 0.55$.

Just as before, the paraboloid of revolution is defined by rotating the function $h_2(r) = c_2 r^2$ around the origin $r = 0$. The equivalent one-dimensional indenter is represented by the parabola $\tilde{h}_2(x) = 2c_2 x^2$. With a given set of parameters, the stationary indentation depth, the contact line and the coefficient of friction can be determined analytically:

$$d = \frac{F_N}{4\eta v}, \quad A_d = \left[0, \sqrt{\frac{F_N}{8c_2 \eta v}}\right], \quad \mu = \frac{2}{3}\sqrt{\frac{2c_2 F_N}{\eta v}} \tag{22}$$

according to Eq. (12), the indenter's geometry, and Eq. (16), respectively.

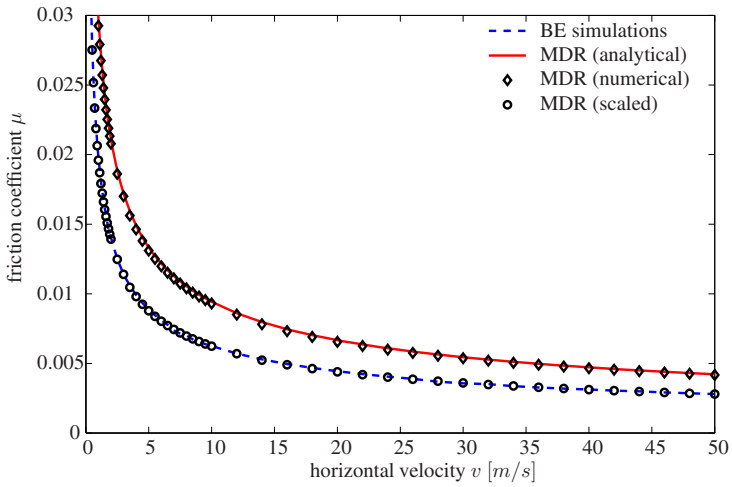

Fig. 8 Comparison of the results obtained by the method of dimensionality reduction (MDR) and by boundary element (BE) simulations. The diagram shows the coefficient of friction as a function of horizontal velocity in the case of a paraboloid of revolution. The results differ by a constant factor only. Thus, the one-dimensional results, scaled by a constant factor of $s_2 \approx 0.67$, nearly coincide with the ones obtained by BE-simulations.

In Fig. 8 the coefficient of friction is plotted as a function of the horizontal velocity. Since both one-dimensional results coincide, they differ from the ones obtained by boundary elements by a constant factor of $s_2 \approx 0.67$. The circles correspond to the one-dimensional results after scaling with this value.

Obviously, both examples support the statement that the results obtained by the method of dimensionality reduction are valid estimations for the original three-dimensional problem. I suppose that the scaling factor s_p is a function of the exponent p of the generating power function $\tilde{h}_p$. But the function is still unknown.

6 Summary

In the present paper a viscous contact problem was used to study the contact of a rigid indenter and a viscoelastic body in the medium frequency range. We used the method of dimensionality reduction to analytically determine the stationary indentation depth and the stationary coefficient of friction. These results exactly hold in reference to the one-dimensional model. Under some assumptions they can also be used as estimates for the original three-dimensional problem. They are reasonable from a dimensional analysis point of view and differ by a constant factor of the order of unity. This is demonstrated with the help of two basic examples and the comparison to boundary element simulations. The approach itself is widely independent of the rheological model and can easily be extended to even more realistic ones.

Acknowledgements The author is grateful to Prof. V. L. Popov for suggesting the topic and valuable guidance. Useful discussions with Dr. R. Heise and B. Grzemba are gratefully acknowledged.

References

[1] I. Argatov, An analytical solution of the rebound indentation problem for an isotropic linear viscoelastic layer loaded with a spherical punch, Acta Mech. **223**(7), 1441–1453 (2012).
[2] Z. Chen and S. Diebels, Parameter re-identification in nanoindentation problems of viscoelastic polymer layers: small deformation, Z. Angew. Math. Mech. **93**(2-3), 88–101 (2013).
[3] R. M. Christensen, Theory of Viscoelasticity: An Introduction (Academic Press, New York, London, 1971).
[4] D. G. Duffy, Green's Functions with Applications (Chapman & Hall/CRC, Boca Raton, 2001).
[5] T. Geike and V. L. Popov, Reduction of three-dimensional contact problems to one-dimensional ones, Tribol. Int. **40**(6), 924–929 (2007).
[6] T. Geike and V. L. Popov, Mapping of three-dimensional contact problems into one dimension, Phys. Rev. E **76**(3), 036710 (2007).
[7] J. M. Golden, Approximate analytic treatment of the problem of a moving ellipsoidal punch on a viscoelastic half-space, Q. J. Mech. Appl. Math. **35**(1), 155–171 (1982).
[8] K. A. Grosch, Relation between friction and visco-elastic properties of rubber, Nature **197**(487), 858–859 (1963).
[9] B. Gross, Mathematical Structure of the Theories of Viscoelasticity, Actualités Scientifiques Industrielles, Vol. 1190 (Hermann, Paris, 1953).
[10] M. Heß, Über die exakte Abbildung ausgewählter dreidimensionaler Kontakte auf Systeme mit niedrigerer räumlicher Dimension, PhD thesis (Technische Universität Berlin, Berlin, 2011).
[11] K. L. Johnson, Contact Mechanics (Cambridge University Press, Cambridge, 1987).
[12] S. Kürschner and A. E. Filippov, Normal contact between a rigid surface and a viscous body: Verification of the method of reduction of dimensionality for viscous media, Phys. Mesomech. **15**(5–6), 270–274 (2012).
[13] S. Kürschner and V. L. Popov, Penetration of self-affine fractal rough rigid bodies into a model elastomer having a linear viscous rheology, Phys. Rev. E **87**(4), 042802 (2013).
[14] L. D. Landau and E. M. Lifschitz, Lehrbuch der Theoretischen Physik, Band VII Elastizitätstheorie (Akademie, Berlin, 1965).
[15] E. H. Lee, Stress analysis in visco-elastic bodies, Q. Appl. Math. **13**(2), 183–190 (1955).
[16] Q. Li, M. Popov, A. Dimaki, A. E. Filippov, S. Kürschner, and V. L. Popov, Friction between a viscoelastic body and a rigid surface with random self-affine roughness, Phys. Rev. Lett. **111**(3) (2013).
[17] S. K. Peddini, C. P. Bosnyak, N. M. Henderson, C. J. Ellison, and D. R. Paul, Nanocomposites from styrene-butadiene rubber (SBR) and multiwall carbon nanotubes (MWCNT) Part 1: Morphology and rheology, Polymer **55**(1), 258–270 (2014).
[18] V. L. Popov and S. G. Psakhie, Numerical simulation methods in tribology, Tribol. Int. **40**(6), 916–923 (2007).
[19] V. L. Popov, Contact Mechanics and Friction: Physical Principles and Applications (Springer, Berlin, Heidelberg, 2010).
[20] V. L. Popov and M. Heß, Methode der Dimensionsreduktion in Kontaktmechanik und Reibung (Springer, Berlin, Heidelberg, 2013).
[21] J. R. M. Radok, Visco-elastic stress analysis, Quart. Appl. Math. **15**(2), 198–202 (1957).
[22] T. Schüler, R. Manke, R. Jänicke, M. Radenberg, and H. Steeb, Multi-scale modelling of elastic/viscoelastic compounds, Z. Angew. Math. Mech. **93**(2–3), 126–137 (2013).
[23] C. M. Segedin, The relation between load and penetration for a spherical punch **4**(02), 156–161 (1957).
[24] I. N. Sneddon, The relation between load and penetration in the axisymmetric boussinesq problem for a punch of arbitrary profile **3**(1), 47–57 (1965).

